Frascati Physics Series Vol. nnn (2001), pp. 000-000
Heavy Quarks at Fixed Target - Rio de Janeiro, Oct. 9-19, 2000

LATEST RESULTS ON ε'/ε FROM NA48

Monica Pepe
CERN, CH-1211 Genève 23, Switzerland
on leave from INFN Sezione di Perugia, 06100 Perugia, Italy
on behalf of the NA48 Collaboration:
Cagliari, Cambridge, CERN, Dubna, Edinburgh, Ferrara, Firenze, Mainz, Orsay, Perugia, Pisa, Saclay, Siegen, Torino, Warszawa, Wien

ABSTRACT

The NA48 experiment at the CERN SPS accelerator aims to measure Re(ε'/ε), the direct CP violation parameter in $K^0 \to 2\pi$ decays, to the precision of 2×10^{-4}. A preliminary result from NA48 based on data collected in 1998 is presented, which combined with the already published NA48 result based on data collected in 1997 becomes: $Re(\varepsilon'/\varepsilon) = (14.0 \pm 4.3) \times 10^{-4}$.

1 Introduction

CP violation has been discovered in the neutral kaons system in 1964 [1] by observing that not only short lived neutral kaons, but also the long lived ones, decay into two pions. This proved that the physical states K_S and K_L do not correspond exactly to CP eigenstates but contain a small admixture ε of the opposite CP state. Besides the state mixing, the interference in the decay amplitudes of different final state isospin may induce direct CP violation, described by the parameter ε'.

The discovery of the third quark family confirmed that the violation of the CP symmetry can also be accommodated into the Standard Model through the imaginary phase in the CKM mixing matrix [2].

The experimental determination of $\mathrm{Re}(\varepsilon'/\varepsilon)$ is done through the double ratio

$$R = \frac{\Gamma(K_L \to \pi^0\pi^0)/\Gamma(K_S \to \pi^0\pi^0)}{\Gamma(K_L \to \pi^+\pi^-)/\Gamma(K_S \to \pi^+\pi^-)} \simeq 1 - 6 \times Re(\varepsilon'/\varepsilon) \tag{1}$$

First evidence of the direct CP violation was observed in 1993 by the NA31 experiment at CERN by measuring $\mathrm{Re}(\varepsilon'/\varepsilon)=(23 \pm 6.5) \times 10^{-4}$ [3]. This observation was not confirmed by the E731 experiment at Fermilab which measured $\mathrm{Re}(\varepsilon'/\varepsilon)=(7.4 \pm 5.2 \pm 2.9) \times 10^{-4}$ [4]. A new generation of experiments in both laboratories was setup to clarify the situation. In 1999 both new experiments presented their results based on the first bunch of their statistics. Both confirmed the existence of direct CP violation: the Fermilab experiment KTeV measured $\mathrm{Re}(\varepsilon'/\varepsilon)=(28.0 \pm 4.1) \times 10^{-4}$ [5] and NA48 at CERN $\mathrm{Re}(\varepsilon'/\varepsilon)=(18.5 \pm 7.3) \times 10^{-4}$ [6]. The final results of these two experiments, with substantially smaller uncertainties, are expected to conclude on the size of the direct CP violation effect and provide a reciprocal cross-check. A third experiment, based on a very different kaon production technique in a collider, KLOE at DAΦNE [7], will help to accomplish this task.

This paper describes the preliminary result from the analysis of NA48 data taken in 1998 which contains $\sim$2.5 times more statistics than the published result based on 1997 data [6].

2 The NA48 method

The measurement of the double ratio R is obtained by counting the number of events in each of the four decay modes. Around five millions of $K_L \to \pi^0\pi^0$, which is the statistically limiting decay mode, are needed to achieve the aimed accuracy of 2×10^{-4} on ε'/ε. This requires a high intensity beam with a powerful trigger and data acquisition systems, as well as a high capacity data storage and data processing farm.

To reduce the systematic biases NA48 takes benefit from the double ratio technique which allows for two fold cancellations: between the charged and the neutral mode and between the K_L and the K_S beams. In order to cope with time varying conditions all four decay modes are collected simultaneously. In such a way beam fluxes and $K_S K_L$ identification inefficiencies cancel between the charged and the neutral modes, and detector, trigger and selection inefficiencies, as well as losses due to accidental activity in the detector, cancel between the K_S and the K_L beams.

In order to minimise the acceptance correction the two neutral beams are nearly collinear and all four decay modes are selected from a common decay region. Since due to the large lifetime disparity the K_S and K_L populate the decay volume in different ways, K_L decays are weighted according to their decay vertex position to match the K_S decay distribution. In this way the K_S and the K_L acceptances become similar and approximately cancel in the double ratio.

High resolution detectors (magnetic spectrometer for charged and liquid krypton electro-magnetic calorimeter for neutral decays) suppress the backgrounds to a sufficiently low level.

The technique described above brings the double ratio of the four raw event counts very close to the final measurement. The influence of slight differences in the K_L and the K_S decay spectra is eliminated by averaging the double ratio in 20 bins of kaon energy. The sum of the corrections needed to account for the residual systematic biases is $\sim 0.5\%$.

3 Experimental setup

3.1 Beam and detector

K_L and K_S beams are produced by the primary 450 GeV proton beam delivered by the SPS accelerator. The beam arrives in pulses ($\sim$2.5 s every 14.4 s) with an intensity of $\sim 1.4 \times 10^{12}$ protons per pulse. Given the different mean decay lengths of K_L and K_S two different production targets are used, located 126 m and 6 m upstream of the beggining of the decay region (Fig. 1). The angle between the proton beam and the K_L production target axis is 2.4 mrad which helps to reduce the neutron admixture in the kaon beam. A bent silicon crystal [8] deflects the proton beam back to the K_L beam direction by channelling and, at the same time, attenuates the beam to $\sim 3 \times 10^7$ ppp which is sufficient to produce enough $K_S \to 2\pi$ decays in the decay volume

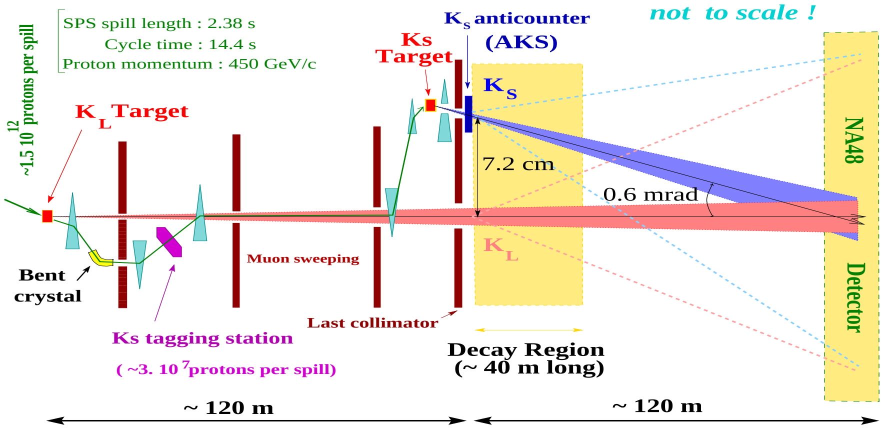

Figure 1: *The layout of the NA48 experiment (side view).*

to match the number of CP violating $K_L \to 2\pi$ decays. The K_S target is placed 7.2 cm above the K_L beam at a production angle of 4.2 mrad, which is chosen to obtain similar K_S and K_L decay spectra. The angle between the K_S and the K_L beams is 0.6 mrad and the beam axes cross at the position of the electro-magnetic calorimeter.

To distinguish K_S and K_L decays the protons directed to the K_S target are detected by the tagging detector [9, 10], an array of scintillator counters placed in the attenuated proton beam just after the bent crystal. The time of flight between the protons and the kaon decay products is measured: the presence or absence of a proton in coincidence with the decay defines the event as K_S or K_L.

The main device for $\pi^+\pi^-$ decay identification is the magnetic spectrometer consisting of four drift chambers and a dipole magnet giving transverse momentum kick of 265 MeV/c. The spatial resolution of $\sim$100 μm per plane results in a momentum resolution of $\sigma_P/P = [0.5 \oplus 0.009 P(GeV/c)]\%$. In order to assure good time measurement for charged particles a scintillator hodoscope is placed between the spectrometer and the LKr calorimeter. Its time resolution of $\sim$200 ps for a $\pi^+\pi^-$ event is important for the K_S tagging.

The neutral decays are reconstructed by a quasi-homogeneus liquid krypton (LKr) electro-magnetic calorimeter with a projective tower readout consisting of $\sim$13500 cells with a lateral size of $2{\times}2$ cm^2. The energy resolution is

$\sigma_E/E = [0.5 \oplus 3.2/\sqrt{E(GeV)} \oplus 10./E(GeV)]\%$, the time resolution for showers above 20 GeV is better than 300 ps and the position resolution is better than 1.3 mm.

Located after the LKr calorimeter are an iron-scintillator hadronic calorimeter and a muon veto counter.

3.2 Trigger

The high beam intensity places strong requirements on the trigger, data acquisition and data recording systems.

The LKr calorimeter is used to trigger on $\pi^0\pi^0$ decays. From horizontal and vertical projections of the energy deposits in the calorimeter the total energy, the decay vertex position and the number of showers are computed to reduce the $\sim$1 MHz particle rate to a $\sim$2 kHz trigger rate with negligible dead time.

The trigger for the $\pi^+\pi^-$ decays consists of two levels. First level is a combination of fast signals from the hodoscope, drift chamber multiplicity and a sum of the energies from both calorimeters. In the second level a processor farm computes the decay vertex position and the invariant mass from the drift chamber signals. The maximum latency of this trigger is 100 μs and the dead time is <5%.

Auxiliary triggers are used to check the performance of the main triggers and to extract control samples.

4 Data analysis

The strategy of the analysis follows the main principle of the NA48 method, which consists in minimisation of the corrections needed to be applied to the double ratio of the raw event counts. This reduces the uncertainties following from the corrections and makes the result robust against unexpected systematic biases. The smallness of the corrections follows from the symmetry in the way the four decay samples are counted.

4.1 Event selection and Backgrounds

All four modes are counted in the same kaon energy interval, $70GeV < E_K < 170GeV$, and decay volume, $0 < c\tau/c\tau_S < 3.5$, where $c\tau$ is the proper decay

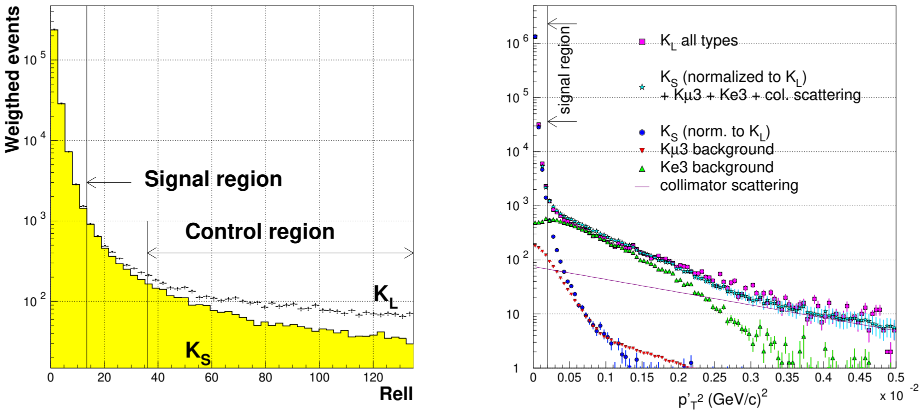

Figure 2: *(a) Distribution of the $R_{ellipse}$ variable for both $K_S \to \pi^0\pi^0$ and $K_L \to \pi^0\pi^0$ candidates. The excess in the K_L tail is due to $K_L \to \pi^0\pi^0\pi^0$ background.*
(b) The distribution of missing transverse momentum ${p'_T}^2$ in charged samples with the background extrapolation.

time and $c\tau_S$ is the K_S lifetime. The dominant source of background in the $\pi^0\pi^0$ mode are $K_L \to \pi^0\pi^0\pi^0$ decays. To select $\pi^0\pi^0$ events four photons are detected in the calorimeter. The longitudinal decay vertex position at the calorimeter D is reconstructed from the energies (E_i) and positions (x_i,y_i) of the showers using the kaon mass (m_K) constraint:

$$D = \sqrt{\sum_{i,j,i>j}^{4} E_i E_j[(x_i - x_j)^2 + (y_i - y_j)^2]}/m_K \tag{2}$$

The invariant masses m_1 and m_2 of the two photons are computed using D and compared to the nominal π^0 mass using a χ^2-like variable

$$R_{ellipse} = \left[\frac{\frac{(m_1+m_2)}{2} - m_{\pi^0}}{\sigma_+}\right]^2 + \left[\frac{\frac{(m_1-m_2)}{2}}{\sigma_-}\right]^2 \tag{3}$$

The invariant mass cut is applied at $R_{ellipse}$<13.5 which corresponds to 3.7 standard deviations. The residual background is estimated from the control region of the $R_{ellipse}$ distribution (Fig. 2a) after subtracting the tail common to both K_S and K_L decays. The extrapolation factor was evaluated by Monte Carlo simulation. The remaining background to signal ratio in the $K_L \to \pi^0\pi^0$ sample amounts to $(6.6 \pm 2.0) \times 10^{-4}$.

In the $\pi^+\pi^-$ mode the semileptonic 3-body K_L decays dominate the background. The K_{e3} channel is suppressed by electron identification comparing the energy in the LKr calorimeter (E) with momentum from the spectrometer (p) and requiring E/p<0.8. In order to symmetrise losses of $\pi^+\pi^-$ candidates this cut is applied to K_S sample as well. In case of $K_{\mu3}$ no associated hit in muon veto counters closer than 4 ns is required. To retain good $\pi^+\pi^-$ events, the invariant mass $m_{\pi\pi}$ should be equal to the kaon mass. A further reduction of the background is obtained using a cut based on the rescaled kaon transverse momentum p'_T, requiring $p'_T < 2 \times 10^{-4}$. The remaining background is subtracted by studying the distributions of well identified K_{e3} and $K_{\mu3}$ samples in the 2-dimensional space of invariant mass and missing transverse momentum. Two control regions are chosen, one dominated by K_{e3} and one by $K_{\mu3}$ decays, and the tail common to both K_S and $K_L \to \pi^+\pi^-$ is subtracted. The relative weight of K_{e3} and $K_{\mu3}$ backgrounds in the residual K_L tail is found and used to extrapolate to the signal region resulting in a background to signal ratio of $(19 \pm 3) \times 10^{-4}$ (Fig. 2b).

4.2 K_S tagging

Despite of the possibility to determine the origin of charged decays (K_S or K_L) through extrapolated vertical decay vertex position, the kaon flavour is determined by tagging in the same way it is done for neutral decays. This makes the measurement to be sensitive only to differences between neutral and charged mistagging probabilities. The event is tagged as K_S if there is a proton within a $\pm 2ns$ coincidence window centered on the event time, otherwise the event is classified as K_L (Fig. 3a).

Two ways of mistagging must be considered: *tagging inefficiency* (α_{SL}) where at least one of the two times was mismeasured, and *accidental tagging* (α_{LS}) due to accidental coincidences between protons in the tagging counter and K_L decays. In the charged mode, these two probabilities can be measured directly by identifying the beam from the extrapolated transversal vertex position. The extrapolation resolution and beam separation are sufficient to determine the kaon flavour with negligible uncertainty. However, in the

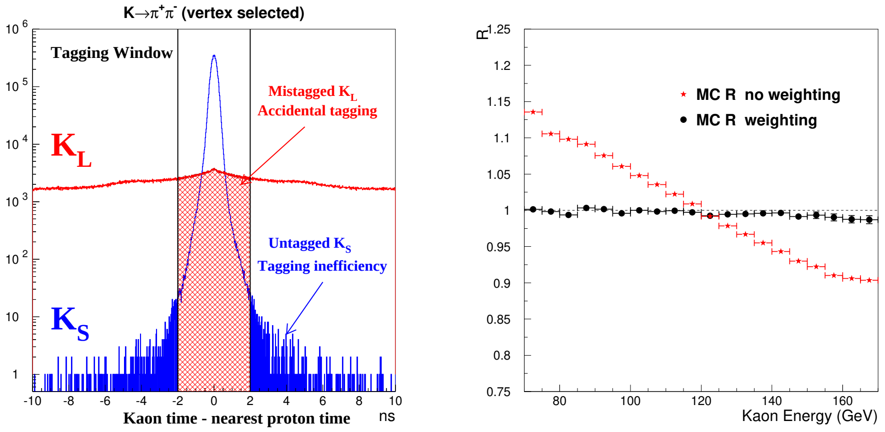

Figure 3: *(a) The distribution of the difference between the time of a $K \to \pi^+\pi^-$ candidate and the nearest proton time detected by the tagging counter. The K_L and K_S contributions are separated by track extrapolation.*
(b) The acceptance correction in bins of kaon energy before and after proper time weighting.

$\mathrm{Re}(\varepsilon'/\varepsilon)$ measurement both charged and neutral modes are treated symmetrically. Therefore the $\mathrm{Re}(\varepsilon'/\varepsilon)$ measurement is sensitive only to differences between the charged and neutral mistagging probabilities. The *tagging inefficiency* measured in the charged mode is $\alpha_{SL}^{+-} = (1.97 \pm 0.05) \times 10^{-4}$. The dominant source of the inefficiency is the tagging counter itself which means that the major part of the inefficiency is symmetric between the charged and the neutral mode. The difference in time reconstruction between $\pi^+\pi^-$ and $\pi^0\pi^0$ is evaluated using $3\pi^0$ decays with one photon conversion: $|\alpha_{SL}^{+-} - \alpha_{SL}^{00}| < 0.5 \times 10^{-4}$, which translates to an uncertainty on the double ratio of $\Delta R < 3 \times 10^{-4}$.

The value of *accidental tagging* probability measured with charged decays is $\alpha_{LS}^{+-} = (11.05 \pm 0.01)\%$: at first order it should be the same for charged and neutral decays, coming from random coincidences in the tagger. To estimate residual effects the difference in proton rates is measured in off-set time intervals, resulting in the correction on the double ratio of $\Delta\mathrm{R} = (1 \pm 8) \times 10^{-4}$.

4.3 Acceptance and proper time weighting

Due to the large differences between the two neutral kaon lifetimes and between the distances of the two targets from the decay volume, the proportion of K_S and K_L decays varies strongly within the common decay region. Since the geometrical acceptance is a function of the distance between the decay vertex and the detector this results in a large acceptance correction on the double ratio of up to 10% depending on the kaon energy. In order to avoid such a large correction, which would require a strong confidence in the precision of the detector description in the acceptance Monte Carlo, the K_L candidates are weighted according to their proper lifetime to match the decay vertex distributions of K_S(Fig. 3b). Thanks to weighting the ratio of the effective event counts between K_S and K_L becomes independent on the decay position and the acceptance correction reduces to a value of $\Delta\mathrm{R} = (+31 \pm 6_{statMC} \pm 6_{syst}) \times 10^{-4}$. The remaining correction reflects mainly the fact that the axes of both beams are not perfectly identical. The advantage of small acceptance correction is, however, payed by a reduction of the statistical significance of the K_L samples. The increase of the statistical uncertainty in the result is $\sim$35 %. The systematic uncertainty on the acceptance correction is conservative and, for the final result, is likely to be improved along with increase of the Monte Carlo statistics.

4.4 Other systematics

One of the basic systematic uncertainties on the measurement of $\mathrm{Re}(\varepsilon'/\varepsilon)$ is the uncertainty on the distance scale that enters the measurement through the definition of the decay region. In order to avoid strong sensitivity to the distance scale uncertainty, the beginning of the decay region is defined by an anti-counter, placed in the K_S beam, instead of using the reconstructed vertex position.

In the neutral decay mode the distance scale is directly related to the energy scale. This is calibrated again by fitting the upstream edge of the $K_S \to \pi^0\pi^0$ vertex distribution. The accuracy of this calibration is 5×10^{-4} which translates to an uncertainty of 3×10^{-4} on the double ratio.

In charged decays the distance scale is defined by the knowledge of the geometry of the first two drift chambers which are used to extrapolate tracks to the vertex. Fitting the upstream edge of the $K_S \to \pi^+\pi^-$ distribution after rejecting all events decaying before the K_S anti-counter a correction on double ratio of $(2 \pm 2) \times 10^{-4}$ was determined.

Other sources of systematic biases are connected to the readout of the electro-magnetic calorimeter and the neutral reconstruction. Their evaluation is based on studies of the $\pi^0\pi^0$ sample and on comparing the response of LKr calorimeter and of the spectrometer for electrons from K_{e3} decays (E/p). Additionally special runs were taken using π^- beam with two polyethylene targets producing high statistics of $\pi^0, \eta \rightarrow \gamma\gamma$ decays which can be used to probe the energy scale, linearity and homogeneity of the LKr calorimeter.

Accidental activity in the detector, which comes mainly from the K_L beam and from the detector noise, can induce losses and gains in the event counts. Two different effects have to be evaluated. One due to difference in the illumination of the detector caused by the difference in the K_S and K_L beam geometry and second, due to variation of the K_S/K_L beam intensity ratio with time (r.m.s. of 10%). The illumination effect was evaluated by overlaying good events with random events, triggered proportionally to the intensity. The measured correction on R is $(2 \pm 6) \times 10^{-4}$. The rest of the effects is absorbed in a limit of $< 10 \times 10^{-4}$ which estimate is based on the knowledge about the size of the dominant contributing effects.

Table 1: *Corrections and systematic uncertainties on the double ratio in the 1997 and the preliminary 1998 results. In order to obtain the effect on Re(ε'/ε) the numbers must be scaled down by factor 6 (Eq. 1).*

	ΔR (Units = 10^{-4})			
Source	1997		1998(prel.)	
Charged trigger	+9	± 23	-1	± 11
Accidental tagging	+18	±9	+1	±8
Tagging efficiency	–	±6	–	± 3
Neutral rec. syst.	–	±12	–	±10
Charged vertex	–	±5	+2	±2
Acceptance	+29	±12	+31	±9
Neutral BKG	-8	±2	-7	±2
Charged BKG	+23	±4	+19	±3
Beam scattering	−12	±3	-10	±3
Accid. activity	-2	±14	+2	±12
Total	+57	±35	+37	±24

5 Result

The 1997 data measurement was based on a sample (after taking into account accidental tagging) containing $0.49 \times 10^6 K_L \rightarrow \pi^0\pi^0$, while the statistics collected in 1998 corresponds to $1.14 \times 10^6 K_L \rightarrow \pi^0\pi^0$.

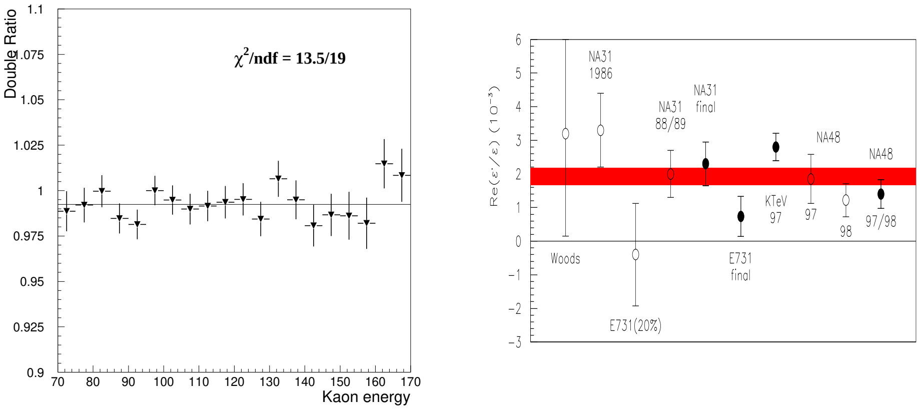

Figure 4: *(a) The stability of the corrected double ratio with kaon energy. (b) Comparison of recent Re(ε'/ε) measurements.*

The list of all corrections applied to the raw double ratio and of all systematic uncertainties is given in the Tab. 1. Many systematic uncertainties are conservative, often dominated by the statistics of the control sample, and will improve in the result from 1999 data.

The stability of the corrected double ratio with changes of the beam and detector conditions, cut variables and kaon energy (Fig. 4a) was checked extensively. The preliminary result obtained from the data collected in the year 1998 is

$$\mathrm{Re}(\varepsilon'/\varepsilon) = (12.2 \pm 2.9_{stat} \pm 4.0_{syst}) \times 10^{-4}. \tag{4}$$

The combined 1997 [6] and 1998 result (after taking into account small correlation in the systematic errors) is

$$\mathrm{Re}(\varepsilon'/\varepsilon) = (14.0 \pm 4.3) \times 10^{-4}. \tag{5}$$

6 Conclusions

The result presented in this paper confirms the existence of the direct CP violation with a positive value of the ε' parameter. The analysis of the 1998 sample is still in progress and the uncertainty on this preliminary result is expected to improve. The analysis of the 1999 data, whose statistics is twice larger, is also in progress. This promises to achieve a total uncertainty on the $\mathrm{Re}(\varepsilon'/\varepsilon)$ measurement of $\lesssim 3 \times 10^{-4}$.

The implosion of the beam pipe by the and of 1999 damaged all four drift chambers and the final run planned for the year 2000 had to be postponed to the year 2001. A part of the 2000 data taking period (without the spectrometer) was used to perform systematics checks on accidental tagging and neutral reconstruction.

Taking into account the three most precise results [3, 4, 5] published up to now and the combined NA48 result the world average is (Fig. 4b):

$$\mathrm{Re}(\varepsilon'/\varepsilon) = (19.3 \pm 2.4) \times 10^{-4}. \tag{6}$$

However the $\chi^2 = 10.5/3$ indicates a very weak consistency among the published results. New results with better accuracy from both KTeV and NA48, as well as first results from KLOE should help to clarify the situation.

References

1. J.H. Christenson *et al*, Phys. Rev. Lett. **13**, 138 (1964).

2. M. Kobayashi and T. Maskawa, Prog. Theor. Phys. **49**, 652 (1964).

3. G.D. Barr et al., Phys. Lett. B **317**, 233 (1993).

4. L.K. Gibbons et al., Phys. Rev. Lett. **70**, 1203 (1993).

5. A. Alavi-Harati et al., Phys. Rev. Lett. **83**, 22 (1999).

6. V. Fanti et al., Phys. Lett. B **465**, 335 (1999).

7. C. Bloise, *these proceedings*.

8. N. Doble et al., Nucl. Instrum. Methods B **119**, 181 (1996).

9. P. Grafström et al., Nucl. Instrum. Methods A **344**, 487 (1994).

10. H. Bergauer et al., Nucl. Instrum. Methods A **419**, 623 (1998).